

RESEARCH ARTICLE

A high-content screen identifies the vulnerability of MYC-overexpressing cells to dimethylfasudil

Jing Zhang¹, Shenqiu Zhang¹, Qiong Shi¹, Thaddeus D. Allen^{1*}, Fengming You², Dun Yang^{1,2*}

1 Anticancer Biosciences and the J. Michael Bishop Institute of Cancer Research, Chengdu, China, **2** Chengdu University of Traditional Chinese Medicine, Chengdu, China

* dun.yang@mbicr.org (DY); thaddeus.allen@mbicr.org (TDA)



OPEN ACCESS

Citation: Zhang J, Zhang S, Shi Q, Allen TD, You F, Yang D (2021) A high-content screen identifies the vulnerability of MYC-overexpressing cells to dimethylfasudil. PLoS ONE 16(3): e0248355. <https://doi.org/10.1371/journal.pone.0248355>

Editor: Irina V. Lebedeva, Columbia University, UNITED STATES

Received: October 16, 2020

Accepted: February 24, 2021

Published: March 24, 2021

Copyright: © 2021 Zhang et al. This is an open access article distributed under the terms of the [Creative Commons Attribution License](https://creativecommons.org/licenses/by/4.0/), which permits unrestricted use, distribution, and reproduction in any medium, provided the original author and source are credited.

Data Availability Statement: All relevant data are within the manuscript and its [Supporting Information](#) files.

Funding: This work was carried out at the private research institute, MBICR (<http://www.mbicr.org/>), with funding through the commercial company, Anticancer Bioscience, Ltd. (ACB) (<https://www.anticancerbio.com/>). J.Z., S.Z., Q.S., T.D.A. and D. Y. are jointly employed by the MBICR and ACB and are paid salary derived from ACB funding. Along with F.Y., individuals mentioned above collectively contributed to study design, data collection and

Abstract

A synthetic lethal effect arises when a cancer-associated change introduces a unique vulnerability to cancer cells that makes them unusually susceptible to a drug's inhibitory activity. The synthetic lethal approach is attractive because it enables targeting of cancers harboring specific genomic or epigenomic alterations, the products of which may have proven refractory to direct targeting. An example is cancer driven by overexpression of MYC. Here, we conducted a high-content screen for compounds that are synthetic lethal to elevated MYC using a small-molecule library to identify compounds that are closely related to, or are themselves, regulatory-approved drugs. The screen identified dimethylfasudil, a potent and reversible inhibitor of Rho-associated kinases, ROCK1 and ROCK2. Close analogs of dimethylfasudil are used clinically to treat neurologic and cardiovascular disorders. The synthetic lethal interaction was conserved in rodent and human cell lines and could be observed with activation of either MYC or its paralog MYCN. The synthetic lethality seems specific to MYC overexpressing cells as it could not be substituted by a variety of oncogenic manipulations and synthetic lethality was diminished by RNAi-mediated depletion of MYC in human cancer cell lines. Collectively, these data support investigation of the use of dimethylfasudil as a drug that is synthetic lethal for malignancies that specifically overexpress MYC.

Significance statement

Synthetic lethal targeting of tumors overexpressing MYC holds promise for attacking aggressive malignancies. Here we describe a synthetic lethal interaction between dimethylfasudil and overexpression of MYC. Uniquely, this novel synthetic lethal interaction points toward an opportunity for synthetic lethality with a molecule likely to harbor favorable drug-like properties that enable systemic use.

Introduction

At least one of the proteins encoded by *MYC*, *MYCN* and *L-MYC*, paralogous members of the MYC family, are deregulated in over 50% of human cancers. This can be due to mutation,

analysis, decision to publish, and preparation of the manuscript. T.D.A. is also affiliated with Tradewind BioScience (TWB). TWB did not contribute funding to this research and holds no commercial interest.

Competing interests: J.Z., S.Z., Q.S., T.D.A. and D. Y. are affiliated with the commercial company Anticancer Bioscience, Ltd. (ACB), which is actively engaged in the development of therapeutics, including a program related to research reported here. ACB has filed the following patent: US20180346995A1 Process for Exploiting Synthetic Lethality Based on OverExpression of MYC Oncogene. T.D.A. is also founder in Tradewind Bioscience, Inc., which holds no interest or ownership in the results presented in this manuscript or the patent listed above.

translocation, amplification or alterations in upstream regulators [1–3]. Alongside binding partners of the MAX family, MYC proteins are recruited to E-box DNA-binding elements [4]. However, MYC is also recruited to non-canonical binding sites and associates with both chromatin modifying and chromatin remodeling complexes and the mediator complex [5]. Pinpointing specific MYC target genes that are absolutely essential for MYC-induced tumorigenesis has proven difficult. One reason is that MYC regulates both tissue and cell-specific gene expression programs [6].

Nonetheless, MYC has been linked to many of the hallmarks of cancer [2, 4] and overexpression of MYC is directly transforming [7]. Several studies have shown that diminishing MYC *in vivo* can elicit tumor regression, suggesting that direct therapeutic targeting of MYC will be a way to attack human malignancies [8–10]. Major challenges exist to developing a drug that directly inhibits MYC. As a transcription factor, MYC functions in the nucleus. Any drug that inhibits MYC may have to gain access to the nuclear compartment, something currently only considered feasible for small molecule drugs. However, unlike kinases, MYC lacks a specific active site for such a small molecule inhibitor to interact. In addition, tumor cell heterogeneity can contribute to the emergence of clones that have acquired additional mutations that allow MYC-independent growth [11]. This means that not all cancer cells with abundant MYC will be absolutely dependent on MYC for proliferation and survival.

One strategy that might overcome all these obstacles is to exploit cellular dependencies uniquely induced by MYC in cancer cells. Such synthetic lethality between overexpression of MYC and targeting of other cellular pathways and proteins has been described with the activation of the DR5 death receptor pathway [12], depletion of the non-essential amino acid glutamine [13], depletion of the core spliceosome component, BUD31 [14], depletion of AMPK-related kinase 5 [15] and pharmacological inhibition of CDK1 [16], PIM1 [17] and Aurora kinase B (AURKB) [18]. Unfortunately, the clinical potential for AURKB inhibitors has been hampered by efficacy and toxicity issues for patients. Toxicity may also limit other synthetic lethal approaches that have not yet advanced to the clinic.

To bypass this possibility, we conducted a phenotypical screen using a small-molecule library of already clinically used drugs and their close analogs for the ability to elicit cell-division defects specifically in MYC overexpressing cells. The high-content screen positively identified a ROCK kinase inhibitor dimethylfasudil (diMF), but not its analogs fasudil and ripasudil. These analogs are themselves ROCK inhibitors so synthetic lethality is mediated by an as yet to be defined target unique to diMF. We utilized both model cell lines and human cancer cell lines to confirm the MYC-diMF synthetic lethal interaction. It was conserved in rodent and human cells and was, in all cases, associated with induction of classical apoptotic features and accumulation of polyploid cells.

Fasudil and ripasudil are both used clinically, with fasudil being used as a systemic treatment. It is likely that diMF may also possess drug-like properties such as a favorable pharmacokinetic and adverse event profile that would enable clinical use. Our findings suggest a new avenue for developing a potent and non-toxic therapeutic intervention for MYC overexpressing tumors using diMF or close chemical analogs with further enhanced properties.

Materials and methods

Cell lines and culture conditions

Human cancer cell lines that were purchased from the American Type Culture Collection (ATCC, Manassas, VA, U.S.A.) include Hela (ATCC[®] CCL-2[™]), NCI-H841 (ATCC[®] CRL-5845[™]), DU-145 (ATCC[®] HTB-81[™]) and Calu-6 (ATCC[®] HTB-56[™]). Cells were grown for three passages and frozen as cell stock. Prior to each experiment, a stock vial was thawed and serially

passed for no more than five generations. As previously described [16], RPE-NEO and RPE-MYC cells were generated by transfecting hTERT-immortalized human primary retinal pigment epithelial cells (RPE-hTERT) with a vector expressing the Neomycin resistance gene (*Neo*) alone or alongside the *MYC* oncogene, respectively, followed by selection with 800 $\mu\text{g/ml}$ G418 (Geneticin). RPE-MYC cells were transfected with a construct harboring an *H2B-GFP* fusion gene and selected with 1 $\mu\text{g/ml}$ of puromycin to generate RPE-MYC^{H2B-GFP} cells for high-content screening. The mammalian *H2B-GFP* expression construct was a gift from Dr. Andrei Goga of the University of California, San Francisco. Construction of derivatives of Rat1A cells and verification of ectopic expression of oncogenic proteins has been described [16, 19]. Briefly, Rat1A cells were infected with retrovirus expressing one of a variety of cancer genes. Transduction efficiency was judged using GFP expression. Rat1A/Myc^{ER}, IMR-90/Myc^{ER}, HA1E/Myc^{ER}, and HA1E/Myc^{N^{ER}} were generated by infection of parental cells with viral particles produced using Phoenix packaging cells (ATCC[®] CRL-3213[™]) followed by puromycin selection (1 $\mu\text{g/ml}$) [13, 20]. All mammalian cells were cultured in DMEM supplemented with 10% fetal bovine serum and antibiotics at 5% CO₂ in a humidified incubator. To ensure that cell lines were free of mycoplasma contamination, a Universal Mycoplasma Detection Kit (ATCC[®] 30-1012K[™]) was used to assay for the mycoplasma 16S rRNA-coding region after experimentation.

Cell viability assays

Cell viability was determined by the trypan blue exclusion assay, as previously described [18], or alternatively through immunofluorescent staining for various apoptotic markers. Viability was expressed as the percentage of dead cells in the population at an indicated time-point following initiation of drug treatment. For each assay, data is presented from three independent experiments that were performed with sequentially passaged cells, and each experiment was done in triplicate ($n = 9$).

Small molecules

The FDA-approved drug panel of 2576 drugs (Cat. # L1300) was purchased from Selleck Chemicals (Houston, TX, U.S.A.). An additional two hundred analogs of various FDA-approved drugs were synthesized in-house and were included in our high-content screening panel. The following small molecules were from commercial sources and used at the final concentrations indicated in the figures or their legends: Rho kinase inhibitor diMF (H1152 dihydrochloride, Cat. # sc-203592) and dihydrocytochalasin B (DCB) (Cat. # sc-202579) were purchased from Santa Cruz Biotechnology (Dallas, TX); fasudil hydrochloride (Cat. # 0541/10) and Y27632 (Cat. # 1254/1) were purchased from Tocris Bioscience (Bristol, U.K.); AZD1152-HQPA (Cat. # S1147), MLN8237 (Cat. # S1133) and VX-680 (Cat. # S1048) were purchased from Selleck Chemicals (Houston, TX); paclitaxel (Cat. # P-9600), etoposide (Cat. # E-4488), staurosporine (Cat. # S-9300) and doxorubicin (Cat. # D-4000) were obtained from LC Laboratories (Woburn, MA); nocodazole (Cat. # M1404), cycloheximide (Cat. # C-7698), cisplatin (Cat. # C2210000) and monastrol (Cat. # M8515) were from Sigma-Aldrich (St. Louis, MO); Zeocin (Cat. # R25001), G418/Geneticin (Cat. # 10131035), 0.4% trypan blue solution (Cat. # 15250061), and puromycin dihydrochloride (Cat. # A1113802) were purchased from Thermo-Fisher Scientific (Waltham, MA); Eg5 inhibitor II (Cat. # BP-30219) was obtained from BroadPharm (San Diego, CA).

High-content drug screening for MYC-synthetic lethal agents

RPE-MYC^{H2B-GFP} cells were cultured in 150 mm petri dishes and were cryo-preserved in large amounts before use. Cells with the same passage number were thawed and seeded to batches

of 96-well microtiter plates with 2,000 cells per well as the starting cell number for high-content screening. Treatment with small molecules was initiated 24 hours after seeding at a final concentration of 10 μ M in 0.1% DMSO. Cells were imaged 24 and 48 hours after initiation of drug treatment to monitor H2B-GFP-labelled DNA using an IN Cell Analyzer 2000 (GE). Compounds that triggered mitotic arrest at 24 hours and polyploidy and apoptosis at 48 hours in RPE-MYC cells, but not RPE-NEO cells, were scored as positive and were subjected to further validation.

RNA interference

Cells were cultured in a 6-well plate and allowed to adhere overnight before transfection with either a negative control siRNA, or *MYC* siRNA at a concentration of 50 nM using Lipofectamine 2000 (Invitrogen) according to the manufacturer's instructions. The sequences for the *MYC* siRNA and control siRNA were previously described [21]. The transfection efficiency was judged by expression of a co-transfected pEGFP-N1 construct (Clontech, now Takara Bio, Mountainview, CA).

Immunofluorescent microscopy

Immunofluorescent staining experiments were performed as previously described [18]. Cells were cultured on coverslips in a 6-well plate, fixed with either 4% paraformaldehyde or 4% paraformaldehyde followed with methanol treatment, and then permeabilized with 0.3% Triton X-100. Rabbit IgG antibodies for active caspase 3 (Cat. # 9661S), active caspase 9 (Cat. # 20750S), and cleaved PARP (Cat. # 5625S) were from Cell Signaling Technology (Danvers, MA) and used at 1:100 dilution. Primary antibodies were detected with Rhodamine (TRITC)-conjugated AffiniPure Donkey Anti-Rabbit IgG (H+L) (Jackson ImmunoResearch, West Grove, PA, Cat. # 711-025-152) at a 1:500 dilution. After immunostaining, we mounted cells on microscope slides with 4',6'-diamidino-2-phenylindole (DAPI)-containing Vectashield mounting solution (Vector Laboratories, Burlingame, CA, Cat. # H1500). For determination of mitochondrial membrane potential, cells were cultured on coverslips and exposed for 30 min. at 37°C with 40 nM Mitotracker™ Red CMXRos (Cat. # M7512) from Thermo-Fisher Scientific, a dye that accumulates in mitochondria as a function of the mitochondrial membrane potential. After fixation in 4% paraformaldehyde, Mitotracker™ Red-stained cells were mounted on microscope slides with DAPI-containing Vectashield. For fluorescence detection, we used either a Zeiss LSM510 confocal laser microscope with a 63X/1.4 N.A. oil objective or an EVOS FL Auto microscope (Thermo-Fisher Scientific).

Time-lapse microscopy

RPE-MYC cells were plated on a 12-well culture dish and treated with vehicle control or drug for 2 hours before conducting live-cell imaging. Bright-field images were captured using an EVOS Auto FL system (Thermo-Fisher Scientific).

Western analysis

Whole cell extracts were prepared by treating cells for 15 min. at 4°C with a lysis buffer (50 mM Tris at pH 7.5, 200 mM NaCl, 0.1% SDS, 1% Triton X-100, 0.1 mM DTT, and 0.5 mM EGTA) supplemented with BD BaculoGold Protease Inhibitor Cocktail (BD Biosciences, San Jose, CA, Cat. # 554779). The extracts were centrifuged at 8,000 \times g for 10 min. to clear insoluble material. The protein concentration in the supernatant was determined using a Bio-Rad Protein Assay (Bio-Rad, Hercules, CA, Cat. # 5000006). Lysates containing 50 μ g of protein

were resolved on NuPAGE (4–12%) Bis-Tris gels (Thermo-Fisher Scientific, Cat. # NP0322PK2) and transferred to nitrocellulose membranes (Bio-Rad, Cat. # 1620150). Equal transfer of protein in each lane was assessed by staining of total protein on the membrane with solution containing 0.1% Ponceau S (w/v) and 5.0% Acetic Acid (w/v) (Sigma-Aldrich, Cat. # P7170-1L). Membranes were then blocked with 5% nonfat milk in PBS buffer for 1 hour before incubating overnight at 4°C with primary antibody diluted 1:1,000 in blocking buffer. Rabbit antibodies against MYC (Cat. # ab32072) and β -ACTIN (Cat. # ab179467) were from Abcam (Cambridge, U.K.) and used at 1:1000 dilution. Horseradish peroxidase-conjugated anti-rabbit immunoglobulins (Santa Cruz Biotechnology, Cat. # sc-2357) were used at 1:5000 dilution. Western blots were visualized with the SuperSignal West Femto ECL detection kit (Thermo-Fisher Scientific, Cat. # 34095).

Blinding of experimental screen and statistical analysis

To reduce observer bias, we blinded the screening experiments. Both the experimenter and statistician were blinded when possible. We randomized the identity of inhibitors with the `RANDBETWEEN` function in Excel and relabeled chemical inhibitors accordingly. Although, chemical identity was blinded, the identity of cell lines was not always blinded to the experimental biologists, because they can distinguish morphological differences among different cell lines. They completed the experiment, and collected data which was statistically analyzed. The identity of cell lines and inhibitors was revealed after completion of statistical analysis.

Statistical analyses were performed with R software. *F* statistics derived from one-way ANOVA were computed using the `aov` function from the `stats` library. The *F* statistics tested the null hypothesis that all group means were equal and were performed at 5% significance level. When null hypothesis of the *F* test was rejected, Dunnett's tests were performed to identify the group means that were statistically different from the control group. Dunnett's two-sided tests were computed using the `DunnettTest` function from the `DescTools` library and were used to compare multiple treatment groups. Two-tailed, unpaired *t*-tests were computed using the `t.test` function from the `stats` library. Each data set represents collective data points from three independent experiments, with three replicates in each experiment ($n = 9$ observations/data point). Error bars represent one standard deviation from the mean. The number of experiments and sample sizes were determined before the collection of any data. In all figures, * indicates significance at a 1% level. The *F* test and Dunnett Test assume normally distributed data. We tested normality of the data with the Shapiro-Wilk's test and failed to reject the null hypothesis of normality in all cases.

Results

Selection of the ROCK inhibitor diMF in a screen for synthetic lethality with MYC

MYC is known to induce potent pro-apoptotic activity but only under specific conditions of cellular stress [1, 22, 23]. We assayed more than 2700 compounds for activity that recapitulated the cellular contexts under which cells could not survive with high levels of the MYC oncogene. Previously, we generated a pair of isogenic cell lines, RPE-NEO and RPE-MYC, by engineering human retinal pigment epithelial (RPE) cells to ectopically express a neomycin resistance gene and the *MYC* oncogene, respectively. This pair of cell lines has been used to demonstrate synthetic lethal interactions between overexpression of MYC and inhibition of either CDK1 [16] or AURKB [18].

Previously, synthetic lethality with the Aurora kinase inhibitor VX-680 has been attributed to the ability of the compound to elicit a transient mitotic arrest and then block cytokinesis [18]. This results initially in apoptosis, but also the eventual accumulation of polyploid cells. Our screen aimed to identify chemicals that can elicit similar cell-division defects. To facilitate screening, a histone *H2B-GFP* fusion gene was stably transfected into cells. This enabled imaging of DNA in live cells. Events were considered positive for synthetic lethality with MYC when cell death was present in RPE-MYC cells, but absent in RPE-NEO cells.

One compound that elicited extensive mitotic arrest at 24 hours and extensive polyplody by 48 hours (Fig 1A) was identified as dimethylfasudil (diMF), (S)-(+)-2-Methyl-1-[(4-methyl-5-quinolinyl)sulfonyl]-hexahydro-1H-1,4-diazepine dihydrochloride, a competitive inhibitor of ROCK kinases. With an IC_{50} of 12 nM for ROCKII inhibition, diMF is considered a potent, selective and reversible ROCK inhibitor. It has only been used in preclinical *in vitro* and *in vivo* studies

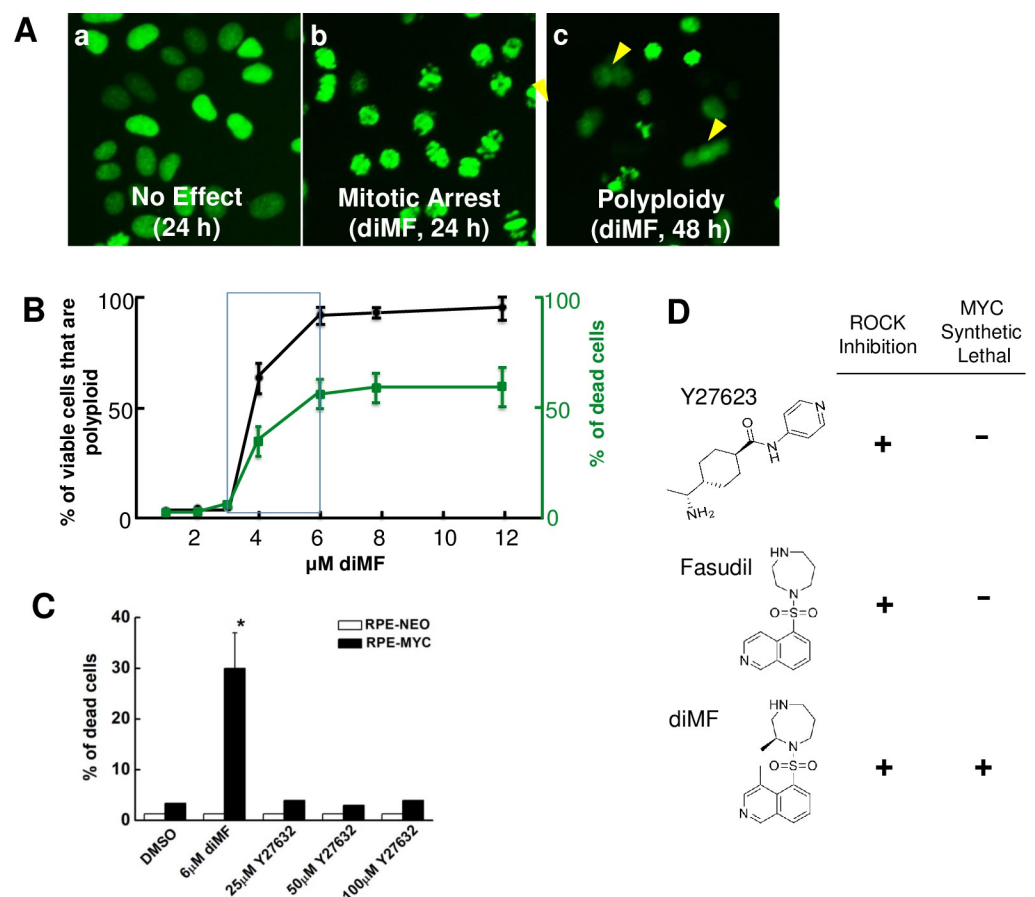


Fig 1. diMF elicits MYC-dependent cytotoxicity. Representative images (A) of RPE-MYC^{H2B-GFP} cell phenotypes observed with high-content screening with a small molecule library. Shown are (a) cells treated with DMSO as a negative control, (b) cells mitotically arrested after 24 hours of diMF (10 μ M) and (c) polyplody cells (arrowheads) that formed after 48 hours of diMF. (B) Concentration-response between diMF and the percentage of non-viable cells after 48 hours (green) and percentage of the remaining cells that are polyplody (black). Data points are derived from experiments done in triplicate from 3 independent experiments (n = 9) and error bars represent standard deviation. (C) RPE-NEO and RPE-MYC cells were treated with vehicle control (0.1% DMSO), diMF (6 μ M) or varying concentrations of the ROCK inhibitor Y27623 for 48 hours. Cell viability was assayed by trypan blue exclusion assay. Viability differences between RPE-NEO and RPE-MYC cells with each chemical were statistically compared using two tailed, unpaired t-tests. The symbol * indicates $p < 0.01$. (D) Comparison of the chemical structure and functional activity of ROCK inhibitors.

<https://doi.org/10.1371/journal.pone.0248355.g001>

[24], perhaps due to the plethora of alternative ROCK inhibitors that have been developed [25]. In confirmatory assays with commercially available compound, diMF induced a concentration-dependent decrease in viability and induction of polyploidy in RPE-MYC cells (Fig 1B).

Additional ROCK inhibitors were also present in the high-content screen, notably fasudil and ripasudil. Both of these clinically used ROCK inhibitors were not found to be synthetic lethal with MYC. To further assay if ROCK inhibition was required for MYC synthetic lethality, we assayed an additional, structurally distinct ROCK inhibitor. The ROCK inhibitor Y27623 could not recapitulate the MYC-dependent synthetic lethality of diMF. Even at a concentration of 100 μM (Fig 1C), Y27623 did not significantly induce cell death in either RPE-NEO or RPE-MYC cells. Thus, diMF alone among the ROCK inhibitors assayed, could selectively induce the death of cells that overexpress MYC (Fig 1D). This likely results from inhibition of an uncharacterized target other than ROCK kinases.

To further explore the induction of polyploidy in diMF treated cells, we used time-lapse microscopy to track drug treated RPE-MYC cell division (Fig 2). Cells were treated with both diMF (5 μM) and fasudil (10 μM). Typically, cells that became polyploid had delayed mitotic progression and commenced cytokinesis, but cytokinetic failure ensued leaving binucleate cells (4n). Polyploid cells formation could only be captured with diMF treatment. Since fasudil is a potent ROCK inhibitor, this strengthens the supposition that diMF induces polyploidy through the inhibition of an alternative target.

diMF-induced death in MYC overexpressing cells is mediated by a mitochondrial apoptotic pathway

To investigate the nature of MYC-dependent death elicited by diMF, we examined the features of diMF-induced cell death in RPE-MYC cells. At least a portion of the cell death phenotype was inhibited by the pan-caspase inhibitor z-VAD-fmk. At 72 hours after 6 μM diMF treatment, z-VAD-fmk at 100 μM provided more than 50% protection against cell death (Fig 3A). Cleaved, or activated, forms of caspases 3 and 9 and the downstream caspase target poly ADP-ribose polymerase 1 (PARP1) were found after diMF treatment (Fig 3B). These features were likely due to activation of mitochondria-dependent apoptosis, since we also could quantify a

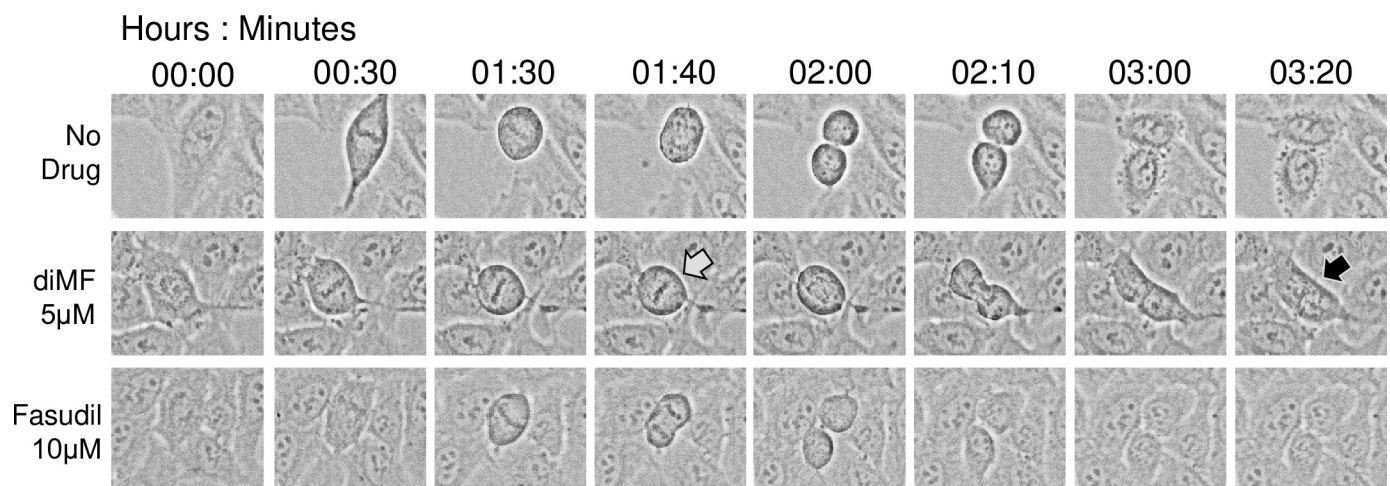


Fig 2. Time-lapse capture of failed cytokinesis with diMF treatment. RPE-MYC cells were captured after treatment with vehicle control, 5 μM diMF or 10 μM fasudil. The grey arrow at time 01:40 denotes a diMF treated cell delayed in mitosis compared to vehicle control cells or cells treated with the ROCK inhibitor fasudil. The black arrow at time 03:20 denotes the same cell which eventually did complete mitosis but failed to complete cytokinesis. The resulting cell was binucleate (4n).

<https://doi.org/10.1371/journal.pone.0248355.g002>

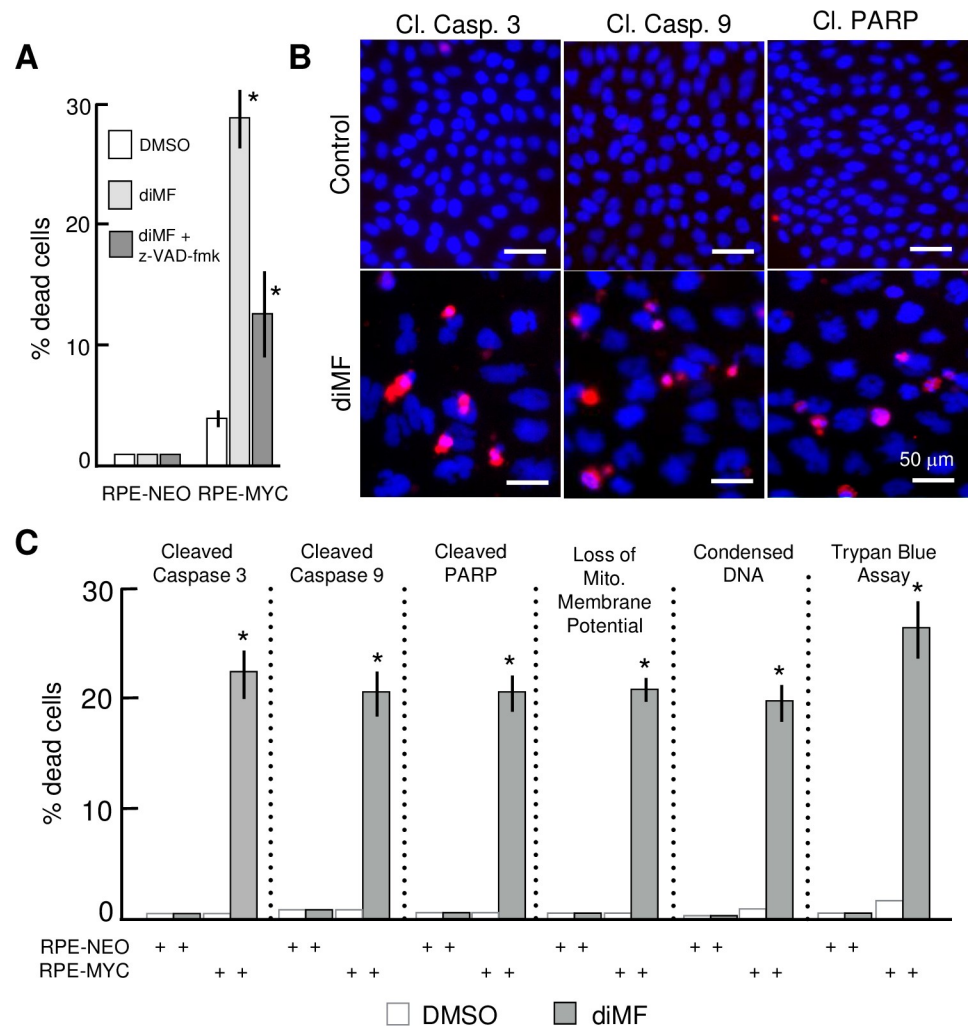


Fig 3. MYC-diMF engages the intrinsic apoptotic cascade for synthetic lethality. (A) Partial inhibition of MYC-diMF synthetic lethality by the caspase inhibitor z-VAD-fmk. RPE-NEO and RPE-MYC cells were treated for 72 hours with 0.1% DMSO (\square), 6 μ M diMF (\blacksquare), or 6 μ M diMF + 100 μ M z-VAD-fmk (\blacksquare). Statistical analysis was with one-way ANOVA followed by Dunnett's test. The symbol * indicates $p < 0.01$ when compared with the DMSO control group. (B) Immunofluorescent staining for cleaved (activated) caspase 3, cleaved caspase 9 and cleaved PARP in RPE-MYC cells treated with 0.1% DMSO (top panels) or 6 μ M diMF (bottom panels) for 3 days. Cells were stained for DNA with DAPI (blue). Micro-images were taken with an EVOS FL Auto microscope. Scale bar, 50 μ m. (C) Percentage of cells positive for cell death markers in the indicated assays. RPE-MYC and RPE-NEO cells were treated with 0.1% DMSO (\square) or 6 μ M diMF (\blacksquare) for 3 days and then subjected to the indicated viability assays. The experiment was done in triplicate so that $n = 9$ for each data point. Error bars represent standard deviation. The symbol * indicates $p < 0.01$ when diMF treatment was compared with DMSO treatment (unpaired, 2-tailed t-test).

<https://doi.org/10.1371/journal.pone.0248355.g003>

diMF-dependent dissipation of the mitochondrial membrane potential, $\Delta\Psi_m$, in RPE-MYC cells (Fig 3C). These observations support the conclusion that at least some of the MYC-dependent, diMF-induced cell death is through a mitochondrial apoptotic cascade.

Acute activation of MYCN also confers susceptibility to the cytotoxicity of diMF

Arguably, the model RPE cell lines used in our experiments have been propagated extensively and it is possible that sustained expression of MYC selected for genetic or epigenetic

alterations that were responsible for the observed interaction with diMF, not MYC itself. To dispel this possibility and also to determine if another MYC paralog could substitute for MYC in the synthetic lethality, we examined sensitivity to diMF in cells expressing MYC^{ER} and MYCN^{ER} fusion proteins, where MYC and MYCN are fused with the estrogen receptor. In these cells, MYC activity is acutely activated by the addition of 4-hydroxy-tamoxifen (4-OH) which induces translocation of oncogenic MYC fusion protein to the nucleus [7]. While both 4-OH and diMF themselves resulted in low but statistically insignificant levels of cell death, the drugs acted synergistically to elicit approximately 30% overall lethality (Fig 4A–4D). This was true with MYC^{ER} in both HA1E (human kidney epithelial cells) and IMR90 (human lung fibroblast) cells. It was also apparent in MYCN^{ER} expressing Rat1a (rat embryo fibroblast) and HA1E cells. We conclude that overexpression of either MYC or MYCN is lethal in combination with diMF, and that the synthetic lethal relationship is conserved in rodent and human cells and both fibroblast and epithelial cell lineages.

Depletion of MYC negates sensitivity to diMF

Human cancers frequently overexpress MYC, but simultaneously may harbor additional mutations, copy number alterations and translocations. The products of these additional

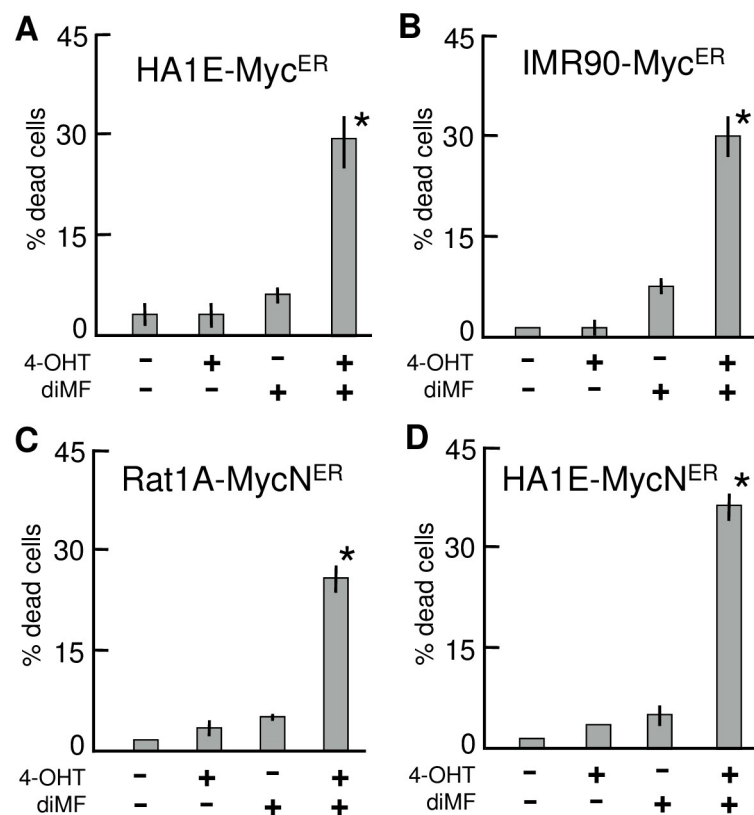


Fig 4. Synergistic induction of cell death by diMF in combination with acute activation of either MYC or MYCN. MYC^{ER} expressing HA1E (A) or IMR90 (B) cells and MYCN^{ER} expressing Rat1A (C) or HA1E (D) cells were incubated with or without 6 μ M diMF and/or 200 nM 4-OHT for 3 days. Cell viability, was determined by the trypan blue exclusion assay. Each column represents the average of three independent experiments with three replicates in each (n = 9). Error bars represent one standard deviation. Statistical analysis was by one-way ANOVA with *p*-values calculated using the Dunnett's test. The symbol * indicates *p* < 0.01 when the indicated double treatment was compared with any of the no treatment or individual treatment groups.

<https://doi.org/10.1371/journal.pone.0248355.g004>

genetic events may mask the synthetic lethality we observed with model immortalized cell lines. We assayed if human cancer-derived cells with abundant MYC were sensitive to diMF and whether overexpression of MYC was necessary for sensitivity. The human cancer lines HeLa (cervical), Calu-6 (lung adenocarcinoma), NCI-H841 (small cell lung cancer) and DU-145 (prostate) are all known to express MYC abundantly and treatment with diMF for four days killed 25–35% of cells with all four of these cell lines (Fig 5A). Next, to assay if MYC was absolutely required for diMF sensitivity, we used RNAi to deplete MYC. MYC protein levels were markedly reduced by MYC RNAi (Fig 5B, full-length Westerns in S1 Fig). Depletion of MYC alone elicited no appreciable levels of toxicity in any of the cell lines (Fig 5C). RNAi depletion of MYC did elicit a more flattened morphology, a change previously reported [21], but cells remained viable. However, depletion of MYC with RNAi did provide each cell line with a 50–75% protection from diMF-induced cytotoxicity (Fig 5D). These findings indicate

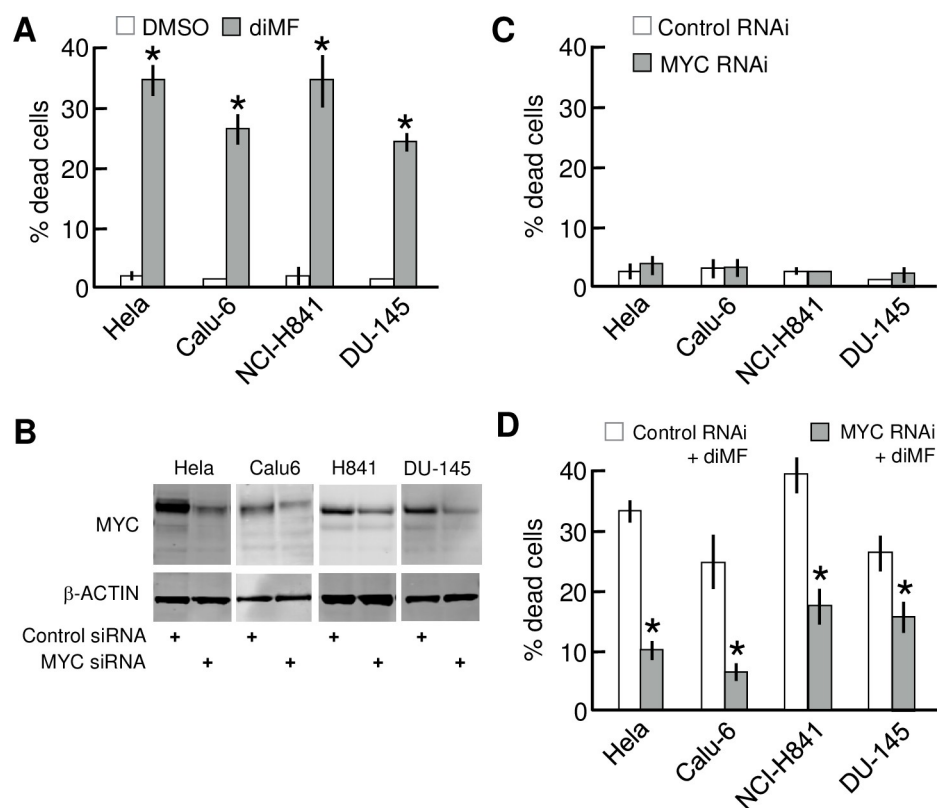


Fig 5. MYC is required in cancer cell lines for cytotoxic killing by diMF. (A) Lethal effect of diMF on a variety human cancer cells that overexpress MYC. Cells were treated with 0.1% DMSO (□) or 6 μM diMF (■) for 3 days. Cell viability was assayed by trypan blue exclusion assay. (B) Depletion of MYC in human cancer cell lines by RNAi. The indicated human cancer cell lines were transfected with either control siRNA (lanes 1, 3, 5, and 7) or MYC siRNA (lanes 2, 4, 6, and 8). Extracts were prepared 3 days after siRNA transfection and Western analysis used to examine levels of MYC and β-ACTIN protein. (C) Depletion of MYC alone fails to elicit cell death. The indicated cancer cell lines were transfected with either control siRNA or MYC siRNA. Cell viability was determined by the trypan blue exclusion assay 4 days after transfection. (D) Suppression of diMF cytotoxicity by RNAi-depletion of MYC. The indicated cancer cell lines were transfected with either control siRNA or MYC siRNA and then exposed to 6 μM diMF starting 24-hours after transfection. Cell viability was determined by the trypan blue exclusion assay at day 4 after transfection. For data in A, C, and D, each data point represents the average of 3 independent experiments with data collected in triplicate (n = 9). Error bars represent the standard deviation. The pairwise comparisons were done using two tailed, unpaired *t*-tests. The symbol * indicates $p < 0.01$ compared to DMSO for A and compared to control RNAi groups in C and D.

<https://doi.org/10.1371/journal.pone.0248355.g005>

that abundant MYC, although dispensable for survival in the absence of diMF, was required for cells to undergo apoptosis in response to diMF.

Alternative oncogenic events do not substitute for MYC in diMF-induced lethality

Our observation with MYC knockdown prompted us to examine more closely if other oncogenic proteins, especially those that influence the cell cycle, might substitute for MYC and confer synthetic lethality with diMF. We assayed the possibility using a panel of rat embryo fibroblasts (Rat1A) that have been engineered to ectopically express a variety of cancer genes [16]. The oncogenic proteins expressed included oncogenic HRAS^{G12V}, myristoylated AKT1 (MyrAKT), BCL-2, ID-1, E2F1, the intracellular domain of NOTCH1 (N1ICD), CYCLIN D1, and BCR-ABL [16]. In a blinded assay, only MYC and the N1ICD-expressing Rat1a cells demonstrated statistically significant cell death with 72 hours of diMF treatment (Fig 6). We concluded that diMF elicited synthetic lethality in combination with MYC and, with the possible exception of the N1ICD, its role could not be substituted by the other oncoproteins assayed. However, N1ICD-diMF lethality was only a fraction of that seen with elevated MYC and diMF treatment and NOTCH1 is a known activator of MYC transcription [26–28]. This regulation may not be conserved in Rat1a cells [19], so whether or not the N1ICD-diMF interaction is a recapitulation of MYC-diMF synthetic lethality has yet to be definitively determined.

Our findings are similar to data obtained in RPE-MYC cells with the pan-Aurora kinase inhibitor VX-680 or an AURKB-specific inhibitor AZD1152 [18]. We recapitulated the findings with VX-680 in the Rat1a panel (Fig 6). Ultimately, synthetic lethality with VX-680 has been attributed to disabling the chromosomal passenger protein complex (CPPC) [18]. Our findings suggest that like VX-680, diMF might somehow disable mitotic spindle assembly, the CPPC or other complexes essential to mitosis, a role not previously ascribed to diMF.

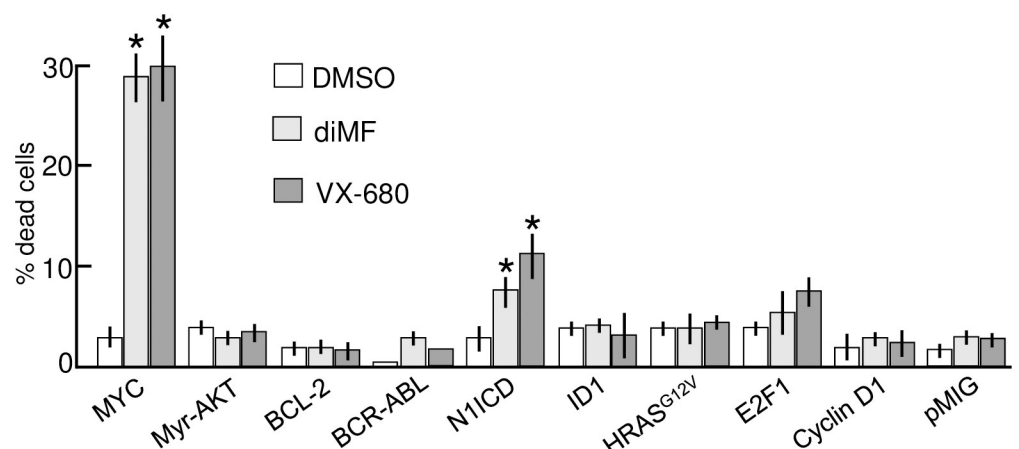


Fig 6. diMF is not synthetic lethal with a variety of other oncoproteins. Rat1A cells harboring either an empty vector or one of the indicated oncogenes, were treated with either 0.1% DMSO (□), 6 μM diMF (▨) or 300 nM VX-680 (■) for 3 days. Cell viability, was assayed using the trypan blue exclusion assay. Each data point is the average of three independent experiments, with treatments done in triplicate (n = 9). Error bars denote standard deviation. For cells overexpressing MYC and the N1ICD, viability of the diMF and VX-680 groups was statistically different from DMSO control (one-way ANOVA followed by Dunnett's test). The symbol * indicates $p < 0.01$ for drug treated compared to DMSO control.

<https://doi.org/10.1371/journal.pone.0248355.g006>

Overexpression of MYC sensitizes cells only to selective apoptotic stimuli

We next asked whether any drug-mediated disturbance of cell division could selectively kill cells that overexpress MYC. We utilized chemical inhibitors to explore four additional means to disturb cell division: (1) stabilizing mitotic spindle microtubules from disassembly with paclitaxel, (2) interfering with the polymerization of microtubules with nocodazole, (3) targeting the centrosomal motor protein Eg5 (also known as KIF11) with monastrol [29], and (4) interfering with assembly of the cytokinesis contractile-ring microfilaments with dihydrocytochalasin B (DCB).

Prevention of cytokinesis with DCB mimicked the selective killing of diMF and VX-680 specifically in RPE-MYC cells (Fig 7). In contrast, paclitaxel and nocodazole killed both RPE-NEO and RPE-MYC. Likewise, inhibition of the centrosomal motor protein Eg5 with either monastrol or Eg5 inhibitor II, both of which prevent separation of centrosomes to form the bipolar mitotic spindle [29], killed cells without discrimination. Both the spindle toxins and Eg5 inhibitors caused prolonged arrest in mitosis prior to apoptotic cell death. In contrast, prolonged arrest in mitosis was not associated with treatment with diMF, DCB and VX-680. It may be that apoptosis in RPE cells following a prolonged arrest in mitosis is not primed by overexpression of MYC, but this is speculative.

A variety of other apoptotic stimuli failed to sensitize RPE-MYC cells to apoptosis. For example, the deoxyribonucleotide synthesis inhibitor hydroxyurea, protein synthesis inhibitor cycloheximide, and serum deprivation all arrested cellular proliferation but caused no cell death in both RPE-NEO and RPE-MYC. Overexpression of MYC sensitized cells to doxorubicin, yet cisplatin and etoposide elicited proliferative arrest, rather than cell death, in both cell lines. Zeocin effectively kills RPE-NEO cells, but not RPE-MYC cells.

Collectively, these data imply that overexpression of MYC does not always prime cells to apoptosis, even with drugs that directly target the mitotic spindle or centrosomes. Doxorubicin which intercalates with DNA and inhibits *topoisomerase II* during DNA replication was preferentially lethal in RPE-MYC cells, but polyploid cells were not induced by this drug and they were induced with diMF. Overall, the data points to a target for diMF that is active at or upstream of the CPPC and functions during cytokinesis.

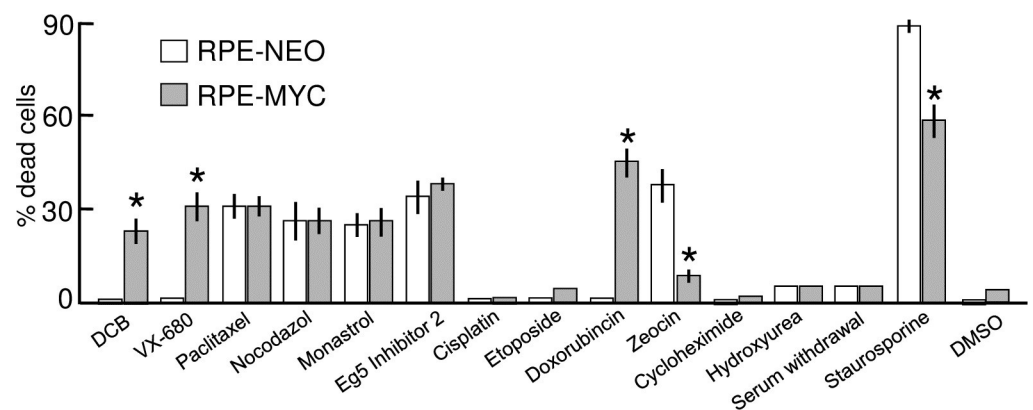


Fig 7. MYC-diMF synthetic lethality is not due to a general priming of apoptosis. Cells overexpressing (RPE-MYC) or not overexpressing (RPE-NEO) MYC were treated for 72 hours with various chemical primers of apoptosis: DCB (2 µg/ml), VX-680 (300 nM), Paclitaxel (5 µM), Nocodazole (1 µg/ml), Eg5 inhibitor II (10 µM), Monastrol (20 µM), Doxorubicin (200 nM), Cisplatin (200 µM), Etoposide (20 µM), Zeocin (50 µg/ml), Cycloheximide (10 µg/ml), Staurosporine (10 µM), serum withdrawal and 0.1% DMSO as a control group. Cell viability was assayed by trypan blue exclusion assay. Each column represents the average of three independent experiments, with three replicates in each experiment (n = 9). Error bars denote standard deviation. Viability differences between RPE-NEO and RPE-MYC cells with each chemical were statistically compared using two tailed, unpaired t-tests. The symbol * indicates $p < 0.01$.

<https://doi.org/10.1371/journal.pone.0248355.g007>

Aurora kinases are not the target of diMF. Inhibition of AURKA or AURKB triggers transient mitotic arrest, polyploidization, and apoptosis of MYC expressing cancer [18, 19, 30], phenotypes reminiscent of those observed here for diMF. To assay whether AURK activity was altered by diMF, RPE-MYC cells were labelled with antibodies recognizing markers associated with AURK activity. Histone 3 phosphorylation at Ser10 was used as a surrogate for AURKB activity. As expected, the AURKB inhibitor AZD1152 inhibited phosphorylation, but a concentration of diMF (12.5 μM) that induces robust apoptosis and polyploidy, did not (Fig 8A). Next, AURKA activity was assayed through examination of AURKA Thr288 phosphorylation. This residue is found in the catalytic domain of the kinase and autophosphorylation results in a significant increase in enzymatic activity [31]. As expected, in cells treated with the AURKA-specific inhibitor MLN8237, signal was lost at spindle poles during cell division (Fig 8B). In contrast, diMF-treated cells maintained robust AURKA Thr288 staining. Our findings suggest that diMF does not inhibit AURKA or AURKB activity at the concentrations used in our assays. An as yet to be identified target mediates diMF-induced synthetic lethality with MYC.

Discussion

MYC contributes to the genesis of many cancers and although it has been a focus of drug research, strategies to target or exploit MYC have yet to be clinically successful. Direct targeting of MYC with small molecule inhibitors may, in fact, be technically impractical. Alternatively, synthetic lethal approaches provide promise to selectively kill tumor cells that overexpress MYC while sparing normal somatic cells [32].

One limitation with current MYC synthetic lethal compounds is toxicity. To circumvent this, we attempted to repurpose existing small-molecule drugs. We carried out phenotypic screening of a small molecule library for MYC-synthetic lethal agents. The well characterized MYC synthetic lethal phenotype elicited by Aurora kinase B inhibitors [18, 19, 33, 34] served as a benchmark for our screen. MYC-VX-680 synthetic lethality, for example, induces

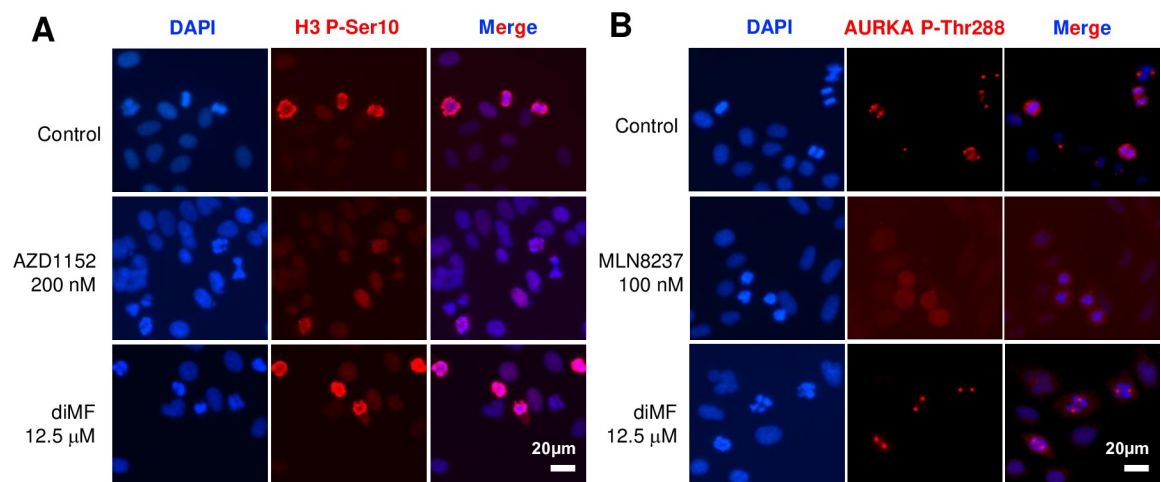


Fig 8. MYC-diMF synthetic lethality is not due to AURK inhibition. (A) Immunofluorescent staining of mitotically arrested RPE-MYC cells for Histone 3 phosphorylated at serine 10 (H3 P-Ser10) as a surrogate for AURKB activity. Staining was at 24 hours of treatment. The AURKB inhibitor AZD1152 (200 nM) was used as a positive control to demonstrate inhibition of phosphorylation. The diMF concentration used (12.5 μM) was previously found to induce maximum cell death and polyploidy. (B) Immunofluorescent staining of RPE-MYC cells for the AURKA activating phosphorylation mark at Threonine 288 (AURKA P-Thr288). Staining was at 24 hours of treatment. The AURKA inhibitor MLN8237 (100 nM) inhibits accumulation of AURKA phosphorylated at Thr288 at the centrosomes of spindle poles. diMF was used at 12.5 μM . DAPI was used as a DNA stain in both (A) and (B).

<https://doi.org/10.1371/journal.pone.0248355.g008>

transient mitotic arrest and apoptosis, followed by induction of polyploidy [18]. The screen uncovered similar activity with a Rho kinase inhibitor, diMF. Our confirmatory experiments showed that this agent selectively elicits lethality with MYC activity. A variety of oncogenic manipulations failed to substitute for MYC in sensitizing cells to diMF. The MYC-diMF synthetic lethality is therefore not a consequence of cellular transformation. In addition, a variety of apoptosis-inducing agents did not preferentially kill MYC-expressing cells, so a general priming of apoptotic signaling by diMF was not responsible for the synthetic lethality either. Instead, diMF likely targets a unique vulnerability induced by MYC overexpression.

ROCK1 and ROCK2 belong to the AGC (PKA/PKG/PKC) family of serine-threonine kinases [25]. diMF has been extensively studied as a ROCK inhibitor and characterized in pre-clinical models. It promotes generation of pancreatic beta-like cells from human pluripotent stem cells [35], augments neurite extension [36], enhances proliferation and migration of endothelial progenitor cells [37] and triggers cell-cycle arrest and cellular senescence of mouse embryo fibroblasts [38]. However, ROCK-independent activity has also been ascribed to diMF. Degradation of polyglutamine-expanded ataxin-3 and 7, causative in spinocerebellar ataxias, is induced by diMF independent of ROCK inhibition [39]. Others have reported non-canonical targets of diMF include LRRK2 [40] and PKA [41]. The MYC synthetic lethality observed here also appears to be ROCK-independent. Other ROCK kinase inhibitors in the screening library, including fasudil and ripasudil, were not identified by our screening effort and later were confirmed negative in eliciting apoptosis and polyploidy in RPE-MYC cells (data not shown).

One report links diMF to mitotic defect and polyploidy. Polyploidy and apoptosis of malignant megakaryocytes can be induced by diMF and this has been ascribed to the inhibition of AURKA [42]. In RPE-MYC cells, MYC synthetic lethality is induced by the AURKB-specific inhibitor AZD1152 [18]. However, diMF does not seem to target AURKs in RPE-MYC cells (see Fig 8). It may be that diMF targets a distinct component or a downstream effector of the CPPC. Nonetheless, we show here that diMF only elicits apoptosis and polyploidy in cells that overexpress MYC. Elucidating diMF targets definitively responsible for this synthetic lethality will require further research.

Fasudil and ripasudil are used clinically and have close structural similarity to diMF. We believe this means diMF will also have drug-like properties; the favorable activity, pharmacokinetic and toxicity profile required for clinical applications. Our findings raise the possibility that diMF might be repurposed for the treatment of MYC overexpressing tumors, which are generally aggressive and may currently lack a targeted therapy option. Alternatively, the diMF structure could serve as the starting point for the synthesis of analogs with improved potency.

Supporting information

S1 Fig. Western analysis of MYC in RNAi-treated cells. The cell lines indicated were treated with control siRNA oligonucleotide or MYC siRNA oligonucleotide, both at a concentration of 50 nM. Levels of MYC (top) and β -ACTIN (loading control, bottom) were assayed by Western analysis to demonstrate knockdown. Band capture is presented in Fig 4B. (TIF)

Acknowledgments

We thank Andrei Goga (University of California, San Francisco) for the Rat1A panel of cells and the H2G-GFP expression construct, Mariia Yuneva (The Francis Crick Institute) for

HA1E/Myc^{ER}, HA1E/MycN^{ER} and IMR90/Myc^{ER} cell lines and Sue Kim (University of Arizona) for the Rat1A/MycN^{ER} cell line.

Author Contributions

Conceptualization: Jing Zhang, Dun Yang.

Data curation: Shenqiu Zhang, Dun Yang.

Formal analysis: Jing Zhang, Shenqiu Zhang, Qiong Shi, Fengming You, Dun Yang.

Funding acquisition: Dun Yang.

Investigation: Jing Zhang, Shenqiu Zhang, Qiong Shi.

Methodology: Shenqiu Zhang, Qiong Shi, Dun Yang.

Project administration: Dun Yang.

Resources: Fengming You, Dun Yang.

Supervision: Fengming You, Dun Yang.

Validation: Jing Zhang, Qiong Shi, Dun Yang.

Visualization: Jing Zhang, Shenqiu Zhang, Qiong Shi, Thaddeus D. Allen, Fengming You, Dun Yang.

Writing – original draft: Thaddeus D. Allen, Dun Yang.

Writing – review & editing: Shenqiu Zhang, Thaddeus D. Allen, Dun Yang.

References

1. Dang CV. c-Myc target genes involved in cell growth, apoptosis, and metabolism. *Mol Cell Biol.* 1999; 19(1):1–11. Epub 1998/12/22. <https://doi.org/10.1128/mcb.19.1.1> PMID: 9858526; PubMed Central PMCID: PMC83860.
2. Gabay M, Li Y, Felsher DW. MYC activation is a hallmark of cancer initiation and maintenance. *Cold Spring Harb Perspect Med.* 2014; 4(6). <https://doi.org/10.1101/cshperspect.a014241> PMID: 24890832; PubMed Central PMCID: PMC4031954.
3. Nesbit CE, Tersak JM, Prochownik EV. MYC oncogenes and human neoplastic disease. *Oncogene.* 1999; 18(19):3004–16. Epub 1999/06/23. <https://doi.org/10.1038/sj.onc.1202746> PMID: 10378696.
4. Dang CV. MYC on the path to cancer. *Cell.* 2012; 149(1):22–35. <https://doi.org/10.1016/j.cell.2012.03.003> PMID: 22464321; PubMed Central PMCID: PMC3345192.
5. Hann SR. MYC cofactors: molecular switches controlling diverse biological outcomes. *Cold Spring Harb Perspect Med.* 2014; 4(9):a014399. Epub 2014/06/19. <https://doi.org/10.1101/cshperspect.a014399> PMID: 24939054; PubMed Central PMCID: PMC4143105.
6. Yuneva MO, Fan TW, Allen TD, Higashi RM, Ferraris DV, Tsukamoto T, et al. The metabolic profile of tumors depends on both the responsible genetic lesion and tissue type. *Cell Metab.* 2012; 15(2):157–70. Epub 2012/02/14. <https://doi.org/10.1016/j.cmet.2011.12.015> PMID: 22326218; PubMed Central PMCID: PMC3282107.
7. Eilers M, Picard D, Yamamoto KR, Bishop JM. Chimaeras of myc oncoprotein and steroid receptors cause hormone-dependent transformation of cells. *Nature.* 1989; 340(6228):66–8. Epub 1989/07/06. <https://doi.org/10.1038/340066a0> PMID: 2662015.
8. Felsher DW, Bishop JM. Reversible tumorigenesis by MYC in hematopoietic lineages. *Mol Cell.* 1999; 4(2):199–207. Epub 1999/09/17. [https://doi.org/10.1016/s1097-2765\(00\)80367-6](https://doi.org/10.1016/s1097-2765(00)80367-6) PMID: 10488335.
9. Jain M, Arvanitis C, Chu K, Dewey W, Leonhardt E, Trinh M, et al. Sustained loss of a neoplastic phenotype by brief inactivation of MYC. *Science.* 2002; 297(5578):102–4. Epub 2002/07/06. <https://doi.org/10.1126/science.1071489> PMID: 12098700.
10. Shachaf CM, Kopelman AM, Arvanitis C, Karlsson A, Beer S, Mandl S, et al. MYC inactivation uncovers pluripotent differentiation and tumour dormancy in hepatocellular cancer. *Nature.* 2004; 431(7012):1112–7. Epub 2004/10/12. <https://doi.org/10.1038/nature03043> PMID: 15475948.

11. D'Cruz CM, Gunther EJ, Boxer RB, Hartman JL, Sintasath L, Moody SE, et al. c-MYC induces mammary tumorigenesis by means of a preferred pathway involving spontaneous Kras2 mutations. *Nat Med*. 2001; 7(2):235–9. Epub 2001/02/15. <https://doi.org/10.1038/84691> PMID: 11175856.
12. Wang Y, Engels IH, Knee DA, Nasoff M, Deveraux QL, Quon KC. Synthetic lethal targeting of MYC by activation of the DR5 death receptor pathway. *Cancer Cell*. 2004; 5(5):501–12. Epub 2004/05/18. [https://doi.org/10.1016/s1535-6108\(04\)00113-8](https://doi.org/10.1016/s1535-6108(04)00113-8) PMID: 15144957.
13. Yuneva M, Zamboni N, Oefner P, Sachidanandam R, Lazebnik Y. Deficiency in glutamine but not glucose induces MYC-dependent apoptosis in human cells. *J Cell Biol*. 2007; 178(1):93–105. Epub 2007/07/04. <https://doi.org/10.1083/jcb.200703099> PMID: 17606868; PubMed Central PMCID: PMC2064426.
14. Hsu TY, Simon LM, Neill NJ, Marcotte R, Sayad A, Bland CS, et al. The spliceosome is a therapeutic vulnerability in MYC-driven cancer. *Nature*. 2015; 525(7569):384–8. <https://doi.org/10.1038/nature14985> PMID: 26331541; PubMed Central PMCID: PMC4831063.
15. Liu L, Ulbrich J, Muller J, Wustefeld T, Aeberhard L, Kress TR, et al. Deregulated MYC expression induces dependence upon AMPK-related kinase 5. *Nature*. 2012; 483(7391):608–12. <https://doi.org/10.1038/nature10927> PMID: 22460906.
16. Goga A, Yang D, Tward AD, Morgan DO, Bishop JM. Inhibition of CDK1 as a potential therapy for tumors over-expressing MYC. *Nat Med*. 2007; 13(7):820–7. <https://doi.org/10.1038/nm1606> PMID: 17589519.
17. Horiuchi D, Camarda R, Zhou AY, Yau C, Momcilovic O, Balakrishnan S, et al. PIM1 kinase inhibition as a targeted therapy against triple-negative breast tumors with elevated MYC expression. *Nat Med*. 2016; 22(11):1321–9. <https://doi.org/10.1038/nm.4213> PMID: 27775705; PubMed Central PMCID: PMC5341692.
18. Yang D, Liu H, Goga A, Kim S, Yuneva M, Bishop JM. Therapeutic potential of a synthetic lethal interaction between the MYC proto-oncogene and inhibition of aurora-B kinase. *Proc Natl Acad Sci U S A*. 2010; 107(31):13836–41. Epub 2010/07/21. <https://doi.org/10.1073/pnas.1008366107> PMID: 20643922; PubMed Central PMCID: PMC2922232.
19. den Hollander J, Rimpi S, Doherty JR, Rudelius M, Buck A, Hoellein A, et al. Aurora kinases A and B are up-regulated by Myc and are essential for maintenance of the malignant state. *Blood*. 2010; 116(9):1498–505. Epub 06/02. <https://doi.org/10.1182/blood-2009-11-251074> PMID: 20519624.
20. Kim S, Chin K, Gray JW, Bishop JM. A screen for genes that suppress loss of contact inhibition: identification of ING4 as a candidate tumor suppressor gene in human cancer. *Proc Natl Acad Sci U S A*. 2004; 101(46):16251–6. Epub 2004/11/06. <https://doi.org/10.1073/pnas.0407158101> PMID: 15528276; PubMed Central PMCID: PMC528940.
21. Liu H, Radisky DC, Yang D, Xu R, Radisky ES, Bissell MJ, et al. MYC suppresses cancer metastasis by direct transcriptional silencing of alpha v and beta3 integrin subunits. *Nat Cell Biol*. 2012; 14(6):567–74. Epub 2012/05/15. <https://doi.org/10.1038/ncb2491> PMID: 22581054; PubMed Central PMCID: PMC3366024.
22. Evan G, Harrington E, Fanidi A, Land H, Amati B, Bennett M. Integrated control of cell proliferation and cell death by the c-myc oncogene. *Philos Trans R Soc Lond B Biol Sci*. 1994; 345(1313):269–75. Epub 1994/08/30. <https://doi.org/10.1098/rstb.1994.0105> PMID: 7846125.
23. Evan GI, Wyllie AH, Gilbert CS, Littlewood TD, Land H, Brooks M, et al. Induction of apoptosis in fibroblasts by c-myc protein. *Cell*. 1992; 69(1):119–28. Epub 1992/04/03. [https://doi.org/10.1016/0092-8674\(92\)90123-t](https://doi.org/10.1016/0092-8674(92)90123-t) PMID: 1555236.
24. Sasaki Y, Suzuki M, Hidaka H. The novel and specific Rho-kinase inhibitor (S)-(+)-2-methyl-1-[(4-methyl-5-isoquinoline)sulfonyl]-homopiperazine as a probing molecule for Rho-kinase-involved pathway. *Pharmacol Ther*. 2002; 93(2–3):225–32. Epub 2002/08/23. [https://doi.org/10.1016/s0163-7258\(02\)00191-2](https://doi.org/10.1016/s0163-7258(02)00191-2) PMID: 12191614.
25. Loirand G. Rho Kinases in Health and Disease: From Basic Science to Translational Research. *Pharmacol Rev*. 2015; 67(4):1074–95. Epub 2015/10/01. <https://doi.org/10.1124/pr.115.010595> PMID: 26419448.
26. Herranz D, Ambesi-Impiombato A, Palomero T, Schnell SA, Belver L, Wendorff AA, et al. A NOTCH1-driven MYC enhancer promotes T cell development, transformation and acute lymphoblastic leukemia. *Nat Med*. 2014; 20(10):1130–7. Epub 2014/09/10. <https://doi.org/10.1038/nm.3665> PMID: 25194570; PubMed Central PMCID: PMC4192073.
27. Hsu KW, Hsieh RH, Lee YH, Chao CH, Wu KJ, Tseng MJ, et al. The activated Notch1 receptor cooperates with alpha-enolase and MBP-1 in modulating c-myc activity. *Mol Cell Biol*. 2008; 28(15):4829–42. Epub 2008/05/21. <https://doi.org/10.1128/MCB.00175-08> PMID: 18490439; PubMed Central PMCID: PMC2493368.
28. Liao WR, Hsieh RH, Hsu KW, Wu MZ, Tseng MJ, Mai RT, et al. The CBF1-independent Notch1 signal pathway activates human c-myc expression partially via transcription factor YY1. *Carcinogenesis*. 2007; 28(9):1867–76. Epub 2007/04/17. <https://doi.org/10.1093/carcin/bgm092> PMID: 17434929.

29. Mayer TU, Kapoor TM, Haggarty SJ, King RW, Schreiber SL, Mitchison TJ. Small molecule inhibitor of mitotic spindle bipolarity identified in a phenotype-based screen. *Science*. 1999; 286(5441):971–4. Epub 1999/11/05. <https://doi.org/10.1126/science.286.5441.971> PMID: 10542155.
30. Zhang J, Zhang S, Shi Q, Allen TD, You F, Yang D. The anti-apoptotic proteins Bcl-2 and Bcl-xL suppress Beclin 1/Atg6-mediated lethal autophagy in polyploid cells. *Exp Cell Res*. 2020; 394(1):112112. Epub 2020/05/31. <https://doi.org/10.1016/j.yexcr.2020.112112> PMID: 32473226.
31. Hirota T, Kunitoku N, Sasayama T, Marumoto T, Zhang D, Nitta M, et al. Aurora-A and an interacting activator, the LIM protein Ajuba, are required for mitotic commitment in human cells. *Cell*. 2003; 114(5):585–98. Epub 2003/09/19. [https://doi.org/10.1016/s0092-8674\(03\)00642-1](https://doi.org/10.1016/s0092-8674(03)00642-1) PMID: 13678582.
32. Dang CV, Reddy EP, Shokat KM, Soucek L. Drugging the 'undruggable' cancer targets. *Nat Rev Cancer*. 2017; 17(8):502–8. <https://doi.org/10.1038/nrc.2017.36> PMID: 28643779; PubMed Central PMCID: PMC5945194.
33. Mollaoglu G, Guthrie MR, Bohm S, Bragelmann J, Can I, Ballieu PM, et al. MYC Drives Progression of Small Cell Lung Cancer to a Variant Neuroendocrine Subtype with Vulnerability to Aurora Kinase Inhibition. *Cancer Cell*. 2017; 31(2):270–85. <https://doi.org/10.1016/j.ccell.2016.12.005> PMID: 28089889; PubMed Central PMCID: PMC5310991.
34. Sos ML, Dietlein F, Peifer M, Schottle J, Balke-Want H, Muller C, et al. A framework for identification of actionable cancer genome dependencies in small cell lung cancer. *Proc Natl Acad Sci U S A*. 2012; 109(42):17034–9. Epub 2012/10/05. <https://doi.org/10.1073/pnas.1207310109> PMID: 23035247; PubMed Central PMCID: PMC3479457.
35. Ghazizadeh Z, Kao DI, Amin S, Cook B, Rao S, Zhou T, et al. ROCKII inhibition promotes the maturation of human pancreatic beta-like cells. *Nat Commun*. 2017; 8(1):298. Epub 2017/08/22. <https://doi.org/10.1038/s41467-017-00129-y> PMID: 28824164; PubMed Central PMCID: PMC5563509.
36. Fuentes EO, Leemhuis J, Stark GB, Lang EM. Rho kinase inhibitors Y27632 and H1152 augment neurite extension in the presence of cultured Schwann cells. *J Brachial Plex Peripher Nerve Inj*. 2008; 3:19. Epub 2008/09/27. <https://doi.org/10.1186/1749-7221-3-19> PMID: 18817543; PubMed Central PMCID: PMC2567309.
37. O E, Lee SW, Lee HS, Lim HS, Ahn HY, Shin JC, et al. Enhancement of endothelial progenitor cell numbers and migration by H1152, a Rho kinase specific inhibitor. *Biosci Biotechnol Biochem*. 2012; 76(1):172–5. Epub 2012/01/11. <https://doi.org/10.1271/bbb.110468> PMID: 22232255.
38. Kumper S, Mardakheh FK, McCarthy A, Yeo M, Stamp GW, Paul A, et al. Rho-associated kinase (ROCK) function is essential for cell cycle progression, senescence and tumorigenesis. *Elife*. 2016; 5:e12994. Epub 2016/01/15. <https://doi.org/10.7554/eLife.12203> PMID: 26765561; PubMed Central PMCID: PMC4798951.
39. Wang HL, Hu SH, Chou AH, Wang SS, Weng YH, Yeh TH. H1152 promotes the degradation of polyglutamine-expanded ataxin-3 or ataxin-7 independently of its ROCK-inhibiting effect and ameliorates mutant ataxin-3-induced neurodegeneration in the SCA3 transgenic mouse. *Neuropharmacology*. 2013; 70:1–11. Epub 2013/01/26. <https://doi.org/10.1016/j.neuropharm.2013.01.006> PMID: 23347954.
40. Nichols RJ, Dzamko N, Hutti JE, Cantley LC, Deak M, Moran J, et al. Substrate specificity and inhibitors of LRRK2, a protein kinase mutated in Parkinson's disease. *Biochem J*. 2009; 424(1):47–60. Epub 2009/09/11. <https://doi.org/10.1042/BJ20091035> PMID: 19740074; PubMed Central PMCID: PMC3759966.
41. Breitenlechner C, Gassel M, Hidaka H, Kinzel V, Huber R, Engh RA, et al. Protein kinase A in complex with Rho-kinase inhibitors Y-27632, Fasudil, and H-1152P: structural basis of selectivity. *Structure*. 2003; 11(12):1595–607. Epub 2003/12/06. <https://doi.org/10.1016/j.str.2003.11.002> PMID: 14656443.
42. Wen Q, Goldenson B, Silver SJ, Schenone M, Dancik V, Huang Z, et al. Identification of regulators of polyploidization presents therapeutic targets for treatment of AMKL. *Cell*. 2012; 150(3):575–89. Epub 2012/08/07. <https://doi.org/10.1016/j.cell.2012.06.032> PMID: 22863010; PubMed Central PMCID: PMC3613864.